MRS Advances © 2017 Materials Research Society
DOI: 10.1557/adv.2017.347

Production and Characterization of Electroactive Nickel Oxides Grown on Nickel Foam by Anodic Oxidation in KOH Melts for Supercapacitor Applications

N. Tokmak [1] and M. Urgen [1]
[1]Istanbul Technical University, Department of Metallurgical and Materials Engineering, 34469, Maslak, Istanbul-Turkey

ABSTRACT

The role of experimental parameters on direct oxidation of nickel foams with anodic oxidation (anodization) in molten KOH and their contribution to capacitance properties are investigated. Temperature of the melt exhibited an important role on the nature of compounds formed by anodic oxidation. On the samples anodized at 280 and 300 °C stoichiometric NiO is formed. Samples anodized in the temperature range of 150-200 °C gave very high maximum currents in CV measurements indicating the formation of electroactive nickel compounds on them. The nature of these compounds is determined as alpha nickel oxy-hydroxide (α-$Ni(OH)_2$) by micro Raman, XRD and FT-IR measurements. Other property that determines the capacity of these electrodes is the morphology of the electroactive layer, which is controlled mainly by the duration of the treatment. 30 minutes of anodic oxidation time is determined as the optimum value. Areal capacity of the samples anodically oxidized at 200 °C for 30 min using 0.8 V cell voltage are determined as 2.73 $F.cm^{-2}$ and 1.58 $F.cm^{-2}$ for 1 $mA.cm^{-2}$ and 20 $mA.cm^{-2}$ discharge current densities respectively.

INTRODUCTION

Nickel oxide/ hydroxide is one of the most promising electrode materials for supercapacitor application due to their electrochemical stability, environmental compatibility and low cost. The different strategies for forming electroactive nickel compounds can be summarized in two groups. First one is the electroactive $Ni(OH)_2$ powder precipitation by chemical, hydrothermal methods followed by mixing with suitable polymer blends [1]. The second one is the production of them on the metallic substrate directly or in-directly. For in-direct production of $Ni(OH)_2$ films, nickel substrates are treated in nickel ion containing solutions using chemical, electrochemical and microwave irradiation methods [2-7]. Synthesis in an autoclave [8-10], molten salt anodization [11], anodic oxidation in by potentiodynamic sweep anodization [12-14] and direct annealing [15] methods are the generally applied routes of production of electroactive $Ni(OH)_2$ layer directly onto the nickel substrate without any usage of external nickel ion source.

Most preferred method is direct oxidation of the metal since the direct electronic contact of electroactive compound with the substrate allows very easy transport of the electrons to the substrate. However, the electroactive nickel compounds are hydroxylated (alpha or beta $Ni(OH)_2$ which is not easily produced by simple heating methods. Electrochemical anodic oxidation conducted in aqueous solutions does not also work satisfactorily for this purpose due to passivation of nickel in alkaline solutions and the requirement of high oxidation potentials. Thus, oxidation studies are generally conducted in hydrogen peroxide containing alkaline solutions in autoclave using high pressures and temperatures in small fixed volumes. However, problems start to arouse by the increase of autoclave volume making the oxidation process uncontrollable

and scale of the method is limited by the size of the reaction vessel [16]. A promising alternative proposed for direct oxidation of nickel substrates is anodic oxidation of them in molten KOH [11]. In this study the role of cell voltage and duration of the process on the capacitative behavior of nickel foams is investigated. However, a detailed systematic study that investigates the role of temperature, morphology and structure of electroactive nickel compounds produced by using this route is not present in the literature.

This study aims to investigate the role of experimental parameters (temperature, cell voltage, time) on the formation and capacity of the electroactive nickel compounds on nickel foam by anodic oxidation in molten KOH. The structural and morphological characteristics of the EA nickel compounds are determined with SEM, XRD, FTIR and micro Raman investigations. Capacity behavior of the samples is determined with conventional cyclic voltammetry and charge discharge measurements.

EXPERIMENTAL

99.99 % purity nickel foam from with 1.6 mm thickness, ≥ 95% porosity (80-110 Pores per Inch. average hole diameters about 0.25mm) and 346 g/m^2 surface density purchased form MTI Corp, CA) are used as substrates prior to the experiments foams are treated with 37% HCl for 5 minutes under ultrasonication followed by rinsing ethanol, acetone and distilled water.

Molten salt treatment is conducted in a ceramic covered graphite crucible (30 mm inner diameter, 70 mm outer diameter and 110 mm length), which also acted as the cathode of the system. Crucible is heated via high frequency induction. Temperature of the system is measured with a thermocouple placed in a hole in the graphite crucible and controlled with a precision of +/-10 °C. A standard regulated DC power supply is used for polarization of the electrodes.

Scanning electron microscope (Jeol 7000F FE-SEM) investigations are conducted to determine the role of anodization parameters (temperature, voltage and time) on the morphology of the formed layers. XRD measurements are realized in glancing incidence mode with an incidence angle of 3 degrees (Cu-Kα radiation) using Philips PW 3710 diffractometer. Micro Raman investigation are carried out using Horiba Jobin Yvon HR800 UV Raman Instrument, using He-Ne laser with 632 nm wavelength. FT-IR Spectrometer with an external reflection module (Bruker Alpha-T) is used for further characterization of the surface layers.

Electrochemical characterizations are conducted using three-electrode configuration. Large area Pt mesh is used as the counter electrode. Potential of the working electrode is measured by a saturated calomel electrode (SCE) using a Luggin capillary. Test are conducted at room temperature using 6 M KOH solution. Charge discharge curves are also obtained in the same electrolyte and electrode configuration.

RESULTS AND DISCUSSION

Effect of the electrolyte temperature on the capacitive behavior

Melting point of dry KOH is 401 °C. However, during melting of analytical grade KOH, it melted at approximately 150 °C indicating that it contains water. Melting point of KOH shows dependence on its water content. Melting point of KOH with a water content of 25% falls to 143 °C [17]. Upon exposing analytical grade KOH to ambient atmosphere its water content increases due its high hygroscopic character. This property of KOH allowed us to conduct anodic oxidation experiments in a temperature range of 150 - 300 °C.

First anodic oxidation experiments are conducted in molten KOH at 300 °C. Using a cell voltage of 0.8 V for 15 minutes. However, the cyclic voltammogram of the nickel foam oxidized in this melt gave low peak currents in cyclic voltammetry measurements (figure 1). Changing the cell voltage in a range of 0.6 to 1.4 V did not make any difference on this behavior

Raman (figure 2) and XRD (figure 3a) measurements conducted on this sample revealed the presence of NiO. This is an expected result since electroactive nickel hydroxides are only stable up to 280 °C and stochiometric NiO starts to form on Ni by heating them above this temperature [18,19].

For the determination of temperature dependency on the capacitive behavior of nickel foam, oxidation experiments are conducted in water containing molten KOH, using a cell voltage of 0.8 V for 15 minutes in a temperature range of 150-280 °C. Cyclic voltammograms obtained from these samples clearly revealed the role of the treatment temperature. It became possible to obtain electroactive nickel hydroxides within a temperature range of 150 - 240 °C. Meaningful peak currents are obtained for the samples treated in the temperature range of 150 – 200 °C (figure 1).

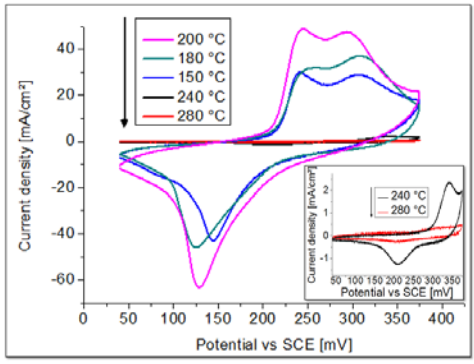

Figure 1. Cyclic voltammograms of nickel foams anodically oxidized at 150-280 °C using a cell voltage of 0.8 V and measured with a scan rate of 20 mV/s in 6 M KOH solution.

For understanding the nature of electroactive nickel compounds formed by anodic oxidation in molten KOH; micro Raman, infrared Spectroscopy and XRD investigations are conducted.

The Raman spectra of the samples that are prepared in the temperature range between 150 – 200 °C gave similar characteristics showing two major peaks at 485 and 566 cm^{-1} that corresponds to the symmetric Ni-OH stretching mode and Ni-O vibration mode [20-22] typical for α-$Ni(OH)_2$ with water containing intercalated structure. The peak at 3580 cm^{-1} that corresponds to symmetric stretching of the hydroxyl groups and generally observed in the Raman spectra of α-$Ni(OH)_2$ powders produced with chemical or hydrothermal methods is not observed. The production route and the resulting disordered crystal structure can be the reason for absence of this peak [23,24]. For samples anodized at 240 °C no distinct Raman shifts are observed highly probably due to incomplete crystallization and highly amorphous structure to

NiO phase at this temperature for samples treated at 280 °C and 300 °C Raman shifts corresponding to NiO are clearly observed at 550 ,1090 and 1490 cm^{-1} [25-27].

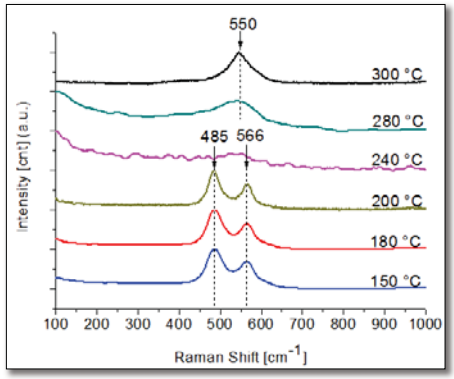

Figure 2. Micro Raman spectra of the anodized Ni –Foams at different temperatures.

For further verifying the nature of electroactive nickel compounds formed on samples treated between 150-200 °C XRD investigations are carried out. In the XRD spectra of the samples treated between 150 -200 °C, small peaks on a broad background corresponding to low diffraction angles were only discernible revealing their low crystallinity and small size (figure 3a). As indicated in the literature, electroactive nickel hydroxide consists of two stable phases which are α -$Ni(OH)_2$ and β-$Ni(OH)_2$. β-$Ni(OH)_2$ is characterized clearly by the help of perfect stacking along the *c* -axis without any intercalated species, while α-$Ni(OH)_2$ is randomly oriented and separated by intercalated water molecules or charge balancing anions (such as NO_3^-, Cl^- and SO_4^{2-}, etc.). Turbostratic disordered structure of this compound reveals itself by the appearance of a broad and poorly crystalline pattern showing low angle reflections and indicates the formation of α -nickel hydroxide [23,28]. Thus, the XRD patterns of the samples anodized in the temperature range of 150-200 °C indicated the formation of α -$Ni(OH)_2$ compound.

Infrared spectroscopy measurements (FT-IR) are also performed over the range 400 – 4000 cm^{-1} (figure 4) to further confirm the Raman and XRD results. The FT-IR spectrum of the sample anodized at 0.8V for 30 min. at 200 °C showed the typical characteristics of α-$Ni(OH)_2$. Seven absorption bands at 3644, 1637, 1463, 1376, 555, 520 and 475 cm^{-1} appear in the spectrum. A broad band centred around 3400 cm^{-1} and ranging from 3800-2500 cm^{-1} corresponds to the presence of hydrogen bonded hydroxyl groups. These double hydroxides spectrum is characteristic of O-H stretching of water molecules and hydroxyl groups in the layered structure [12,28]. The weak bands around 1000 – 1500 cm^{-1} indicates presence of anions in sample [28]. The peak at around 1637 cm^{-1} is attributed to angular deformations of water molecules [12,20]. The band at 1376 cm^{-1} can be attributed to the C=O vibration of the absorbed CO_2 molecules [20], and the peak at 1463 cm^{-1} could be assigned as carbonate ions caused by dissolution of CO_2 from air. A major peak at 555 cm^{-1}, and two small peaks at 475, 520 cm^{-1} corresponds to Ni-O-H vibrations. The peak at 475cm^{-1} is assigned to the Ni-O stretching vibration [23].

Results of the characterization works, clearly revealed that it is possible to form electroactive α-$Ni(OH)_2$ compound by the anodization of nickel foams in a temperature range of 150-200 °C in molten KOH. The chemical nature of the compounds formed in this temperature range did not exhibit any appreciable difference. These, disordered electrode materials with turbostratic structure and large interlayer spacing, low crystallinity and highly dense grain boundaries are preferable for supercapacitor electrode materials due to their higher interaction with the electrolyte leading to an enhancement of energy storage performance [12,29].

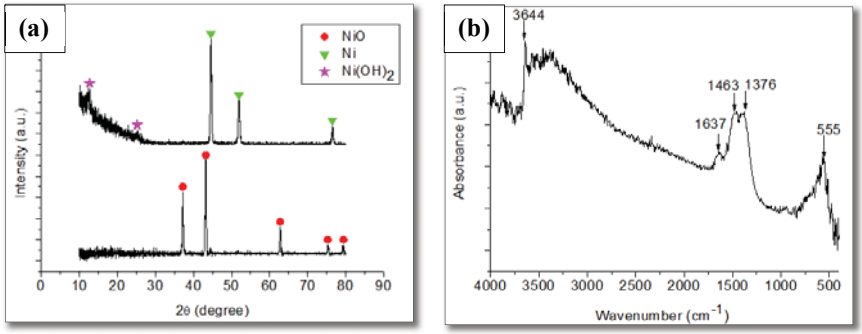

Figure 3. (a) Representative XRD pattern of samples anodized below 240 °C and at 300 °C (b) Representative FT-IR spectrum of samples anodized below 240 °C.

Since the chemistry of the electroactive compounds formed in the temperature range of 150-200 °C are similar, the differences between the capacitive behavior of the samples anodized at different temperatures can be attributed to the morphology, distribution, thickness and coverage of these compounds on nickel foam. For understanding anodizing temperature dependent differences on the morphology of the electroactive compounds, FE-SEM investigations are carried out (figure 4).

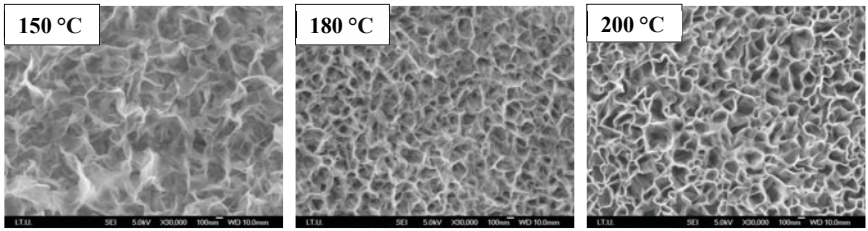

Figure 4. Temperature dependent morphology of the electroactive nickel hydroxides produced by using 0.8 V cell voltage for 15 min.

Upon anodization of nickel foam sponge like structures with nanoscale features starts to form on them. This morphology is similar to morphologies of electroactive nickel powders obtained by chemical or hydrothermal methods [8-10]. This similarity indicates that the formation of these structures is following the same route. Thus, electroactive compounds form after dissolution of nickel in ionic form and followed by its precipitation as Ni hydroxides after reacting with the hydroxyl ions [30]. By the increase of the anodization temperature the height of flakes and the surface area of the layer increases (Fig.4). Better capacitive behavior of samples anodized at 200 °C can be attributed to an increase in the surface area of the electroactive α-$Ni(OH)_2$.

Effect of cell potential on the capacitive behavior

To understand the effect of anodization voltage on capacitive behavior, experiments were carried out between 0.4 - 1.4 V for 15min at 200 °C. For samples anodized at 0.4 V, low peak currents (1 $mA.cm^{-2}$) in CV measurements are obtained. On the other hand, for samples anodized at 1.4 V, thickness of the layer increased dramatically resulting in flaking and spalling of the layer from the surface.

It became possible to obtain durable surface layers for samples anodized in a voltage range of 0.6-1.2 V. 0.8 V cell voltage is selected as the optimum parameter since the highest peak current in CV is achieved by anodizing nickel foam at this potential as shown in figure 5.

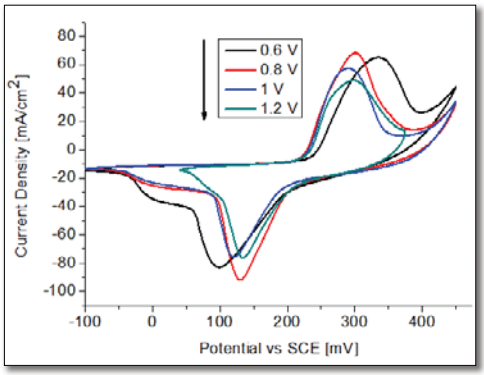

Figure 5. Cyclic voltammograms of nickel foams anodically oxidized at 200 °C using a cell voltages between of 0.6 to 1.2 V and measured with a scan rate of 20 mV/s in 6 M KOH solution.

Effect of the anodization duration on the capacitive behavior

The role of the anodization time on the capacitive behavior are investigated for samples anodized at 0.8 V, 200 °C for 15, 30, and 60 mins. The flaky structure became more evident for samples anodized for 30 and 60 min (figure 6) that reflected its influence on the CV curves (figure 7). Although the sample treated for 60 min exhibited the highest capacitance, it started to spall during CV measurements highly probably due to its high thickness (figure 8). Thus 30 min was selected as the optimum time due to its good sustainability and adherence properties.

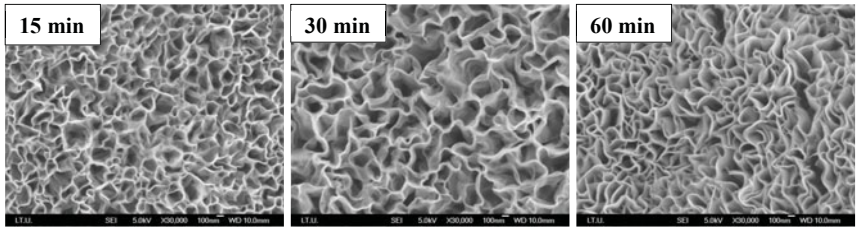

Figure 6. Time dependent morphology of the electroactive nickel hydroxides produced by using 0.8 V cell voltage at 200 °C for 15, 30 and 60 min

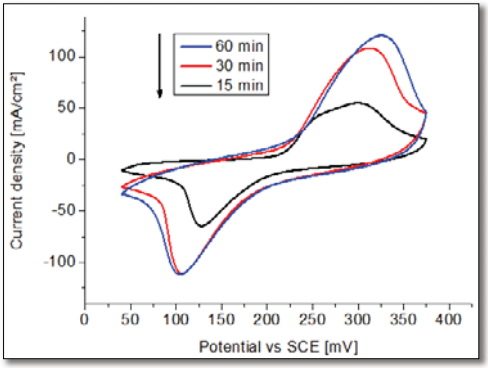

Figure 7. Cyclic voltammograms of nickel foams anodically oxidized at 200 °C, anodized for 15,30 and 60 min. and measured with a scan rate of 20 mV/s in 6 M KOH solution.

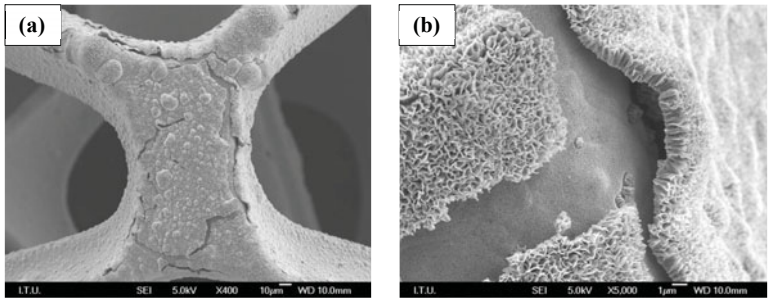

Figure 8. SEM micrographs of the nickel foam anodized at 0.8 V and 200 °C for 60 min . a) general view b) closer view of cracked areas

Charge –discharge behavior

Samples produced by the optimized parameters (anodized with 0.8 V cell voltage, for 30 min. at 200 °C) are used for the determination of charge discharge behavior. Before determining their charge discharge behavior scan rate dependent CV curves are obtained (figure 9).

In order to evaluate the charge discharge behavior of the samples discharge current dependent discharge times are obtained from which areal capacity is calculated (figure 10).

Highest (2.74 $F.cm^{-2}$) and lowest (1.58 $F.cm^{-2}$) areal capacitance values are achieved for the lowest (1 $mA.cm^{-2}$) and highest (20 $mA.cm^{-2}$) discharge currents.

For the determination of cycling stability, charge – discharge behavior of the sample is determined after subjecting to 1000 cycles with CV test. An areal capacitance value of 2.2 F/cm^2 is calculated for a discharge current of 1 $mA.cm^{-2}$. This result revealed that the electrode exhibits excellent cycling stability with maintaining 80.6 % of its capacity after 1000 cycles.

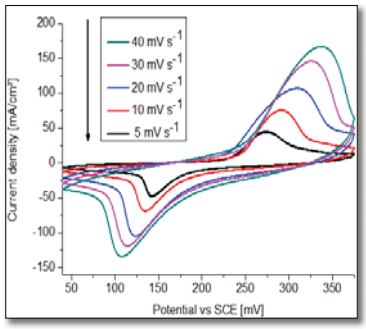

Figure 9. CV Curves of obtained with various scan rates ranging from 5 mVs^{-1} to 40 mVs^{-1}

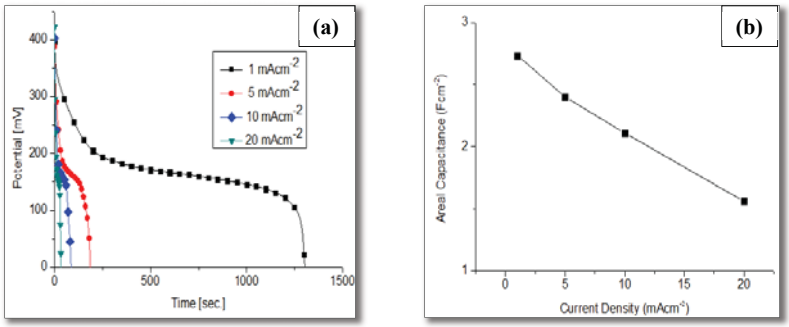

Figure 10. (a) Galvanostatic charge-discharge curves at various current densities ranging from 1 $mAcm^{-2}$ to 20 $mAcm^{-2}$, (b) The areal capacitance values at various current densities ranging from 1 $mAcm^{-2}$ to 20 $mAcm^{-2}$

CONCLUSIONS

Results of the study clearly revealed that it is possible to produce electroactive nickel compounds on nickel foam by anodizing them in molten KOH. Temperature of the melt is the most significant parameter for obtaining electroactive nickel compounds on them. For samples anodized above 240 °C NiO, exhibited very low capacity due to the formation of stoichiometric NiO. On the other hand, on the samples anodized in a temperature range of 150-200 °C nickel compounds giving appreciable maximum currents in CV experiments conducted in 6 M KOH are formed. The nature of the electroactive nickel compound is determined as α-$Ni(OH)_2$ with micro-Raman, XRD and FT-IR measurements. Morphology of the EA nickel compounds that showed dependence on the duration of the anodization process is another parameter that is effective on their capacity. Sponge like structure with nano features becomes more apparent with the increase of anodization time. However, anodization for longer times led to the thickening and spalling of the EA layer from the surface.

Charge discharge behavior of the electrode produced under optimum conditions determined in this study, showed that it is possible to obtain high areal capacitance values by using this oxidation method. Additionally, these electrodes retained %80.6 of their initial capacity after 1000 cycles. Areal capacitances, (calculated from charge –discharge curves using different discharge currents) ranging between 1.76 to 2.74 $F.cm^{-2}$ are obtained. These values are lower that the areal capacity obtained by using this method (4.74 $F.cm^{-2}$) [11], this difference can be attributed to the differences in the surface area of the nickel foams.

Some recent results from the literature on areal capacitances of Ni-O based electroactive films produced by binder free processes in are presented in Table 1. Although there are very high reported areal capacitances, these are attained by the introduction of additional ingredients and substrate surface modifications that led to a substantial increase in surface area and load of electroactive oxides [33,35,36]. The areal capacitance of Ni-O electroactive materials grown on nickel foam without additional ingredients ranged between 0.27-4.74 F. cm^2. The capacitances obtained in this work and the other work [11] that used the same process are among the highest ones.

Table 1. **Areal Capacitances** of Ni-O based electroactive films produced by binder free processes

Electrode Material	Areal Capacitance ($F.cm^{-2}$)
NiO [31]	0.27
$Ni(OH)_2$/Ni Foam [32]	0.45
$Ni(OH)_2$/Ni Foam [33]	0.70
NiO Nanosheets/Ni Foam [11]	4.74 (@4 $mA.cm^{-2}$)
RGO/ $Ni(OH)_2$/Ni Foam [32]	2.5 (@5 $mA.cm^{-2}$)
CNT@ $Ni(OH)_2$/Ni Foam [33]	16
Co_3O_4@NiO/Ni Foam [34]	2.56
Co_3O_4/$Ni(OH)_2$/Ni Foam [35]	15.83 (@2.5 $mA.cm^{-2}$)
Pyrolytic Graphite/ $Ni(OH)_2$ [36]	5.2 (@2 $mA.cm^{-2}$)

ACKNOWLEDGMENTS

This study is supported financially by 115M129 – TUBITAK 1001 Project and tales part in 2515 COST Action, MP1407. Support of Dr. Güldem Kartal during setting up molten salt electrolysis set-up is gratefully acknowledged.

REFERENCES

1. J. Li, F. Luo, Q. Zhao, Li, Z., H. Yuan and D. Xiao, *J. Mater. Chem. A*, *2*(13), 4690-4697, (2014).
2. L.A. Saghatforoush, M. Hasanzadeh, S. Sanati and R. Mehdizadeh, *Bull. Korean Chem. Soc.*, *33*(8), 2613-2618, (2012).
3. P. Haring, and R. Kotz, *J. Electroanal. Chem.*, *385*(2), 273-277, (1995)
4. L. Gu, Y. Wang, R. Lu, L. Guan, X. Peng, and J. Sha, *J. Mater. Chem. A*, *2*(20), 7161-7164, (2014).
5. M.S. Wu, Y.A. Huang, J. J. Jow, W. D. Yang, C. Y. Hsieh, and H. M Tsai, *Int. J. Hydrogen Energy*, *33*(12), 2921-2926, (2008).
6. K. Wang, L. Li, and T. Zhang, *Int. J. Electrochem. Sci., 8*(5), 6252-6257, (2013).
7. Y. Zhu, C. Cao, S. Tao, W. Chu, Z. Wu and Y. Li, *Sci. Rep.*, *4*, 5787, (2014).
8. S. Ni, X. Lv, J. Ma, X. Yang and L. Zhang, *J. Power Sources*, *270*, 564-568, (2014).
9. L. Li, J Xu, J. Lei, J. Zhang, F. McLarnon, Z. Wei and F. Pan, *J. Mater. Chem. A*, *3*(5), 1953-1960, (2015).
10. L. Kumari, and W. Z. Li, *Phys. E, 41*(7), 1289-1292, (2009).
11. L. Yang, L. Qian, X. Tian, J. Li, J. Dai, Y. Guo and D. Xiao, *Chem.– Asian J., 9*(6), 1579-1585, (2014).
12. G. Zhang, W. Li, K. Xie, F. Yu and H. Huang, *Adv. Funct. Mater.*, *23*(29), 3675-3681, (2013).
13. M. Jin, G. Zhang, F. Yu, W. Li, W. Lu and H. Huang, *Phys. Chem. Chem. Phys*, *15*(5), 1601-1605, (2013).
14. M. M. Chen, X. B. Xiong, C. Yi, J. Ma and X. R. Zeng, *J. Inor. Organomet. Polym. Mater., 25*(4), 739-746, (2015).
15. J. L. Yin and J. Y. Park, *Int. J. Hydrogen Energy*, *39*(29), 16562-16568, (2014).
16. D. S. Hall, D. J. Lockwood, C. Bock, B. R. MacDougall. *Proc. R. Soc. A471: 20140792,* (2015).
17. W. F. Linke, A. Seidell, Vol. 2, 4th Ed., *ACS Pub.,* 1965, pp. 276.
18. V. Srinivasan and J. W. Weidner, *J. Electrochem. Soc.*, *147*(3), 880-885, (2000).
19. Y. Fan, Z. Yang, X. Cao, P. Liu, S. Chen, Z. Cao, *J. Electrochem. Soc.* 161, B201–B206, (2014)
20. H. B. Li, M. H. Yu, F. X. Wang, P. Liu, Y. Liang, J. Xiao and G.W.Yang, *Nat. Commun.*, *4*, 1894 (2013)
21. Y. L. Lo and B. J. Hwang, *Langmuir*, *14*(4), 944-950, (1998).
22. B. S. Yeo and A. T. Bell, *J. Phys. Chem. C*, *116*(15), 8394-8400, (2012).
23. G. R. Fu, Z. A. Hu, L. J. Xie, X. Q. Jin, Y. L. Xie, Y. X. Wang and H. Y. Wu, *Int. J. Electrochem. Sci*, *4*(8), 1052-1062, (2009).

24. X. H. Xiong, Z. X. Wang, H. J. Guo and X. H. Li, *Mater. Lett.*, *138*, 5-8, (2015).
25. N. Mironova-Ulmane, A. Kuzmin, I. Steins, J Grabis, I. Sildos and M. Pärs. In *Journal of Physics: Conference Series* (Vol. 93, No. 1, p. 012039). IOP Publishing, (2007).
26. W. J. Duan, S. H. Lu, Z. L. Wu and Y. S. Wang, *J. Phy. Chem C*, *116*(49), 26043-26051, (2012).
27. S. S. Chan and I. E. Wachs, I. E, *J. Catal.*, *103*(1), 224-227, (1987).
28. R. Acharya, T. Subbaiah, S. Anand and R. P. Das, *Mater. Lett.*, *57*(20), 3089-3095, (2003).
29. L. Feng, Y. Zhu, H. Ding and C. Ni. *J. Power Sources*, *267*, 430-444. (2014).
30. Y. Miao, L. Ouyang, S. Zhou, L. Xu, Z. Yang, M. Xiao, M. and R. Ouyang, *Biosens. Bioelectron.*, *53*, 428-439, (2014).
31. A. Armutlulu, J. K. Kim, M. Kim et al. *Proc.of Transducers&Eurosensors XXVII Conf.,* 1480–1483 (2013).
32. S. Min, C. Zhao, G. Chen, X. Qian, *Electrochim. Acta*,115, 155–164, (2013).
33. Z. Tang, C.H. Tang, H. Gong*, Adv. Funct. Mater*, 22, 1272–1278, (2012).
34. X. Xia, J. Tu, Y. Zhang, X. Wang, C. Gu, X.B. Zhao, H.J. Fan, *ACS Nano*, 6, 5531–5538, (2012).
35. C.H. Tang, X. Yin, H. Gong, *ACS Appl. Mater. Interfaces*, 5, 10574–10582, (2013).
36. S. Shahrokhian, R. Mohammadi, M.K. Amini, *Electrochim. Acta,* 206, 317–327, (2016).